

## Isotopic shifts in $^3P$ states of the carbon atom

Saeed Nasiri<sup>a</sup>, Sergiy Bubin<sup>a</sup> and Ludwik Adamowicz<sup>b,c</sup>

<sup>a</sup>Department of Physics, Nazarbayev University, Nur-Sultan, Kazakhstan; <sup>b</sup>Department of Chemistry and Biochemistry, University of Arizona, Tucson, AZ, USA; <sup>c</sup>Department of Physics, University of Arizona, Tucson, AZ, USA

### ABSTRACT

Isotope shifts in the transition energies between several lowest  $^3P^e$  states of the carbon atom are calculated at the nonrelativistic level of theory. We considered the  $^{12}\text{C}$ ,  $^{13}\text{C}$ , and  $^{14}\text{C}$  isotopes, for which we performed variational calculations by expanding the wave functions of the atomic states in terms of all-electron explicitly correlated Gaussian functions. The Born–Oppenheimer approximation was not assumed in the calculations. By combining the computed isotope shifts with the experimentally derived Ritz wavelengths for the natural mixture of the isotopes we make predictions of the positions of the spectral lines for specific carbon isotopes. These predictions may be useful for guiding future experimental measurements of these lines using high-resolution spectroscopy.

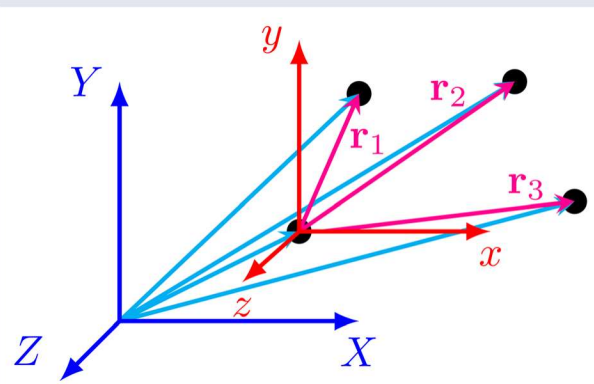
### ARTICLE HISTORY

Received 20 December 2023

Accepted 23 February 2024

### KEYWORDS

Isotope shift; carbon atom; explicitly correlated Gaussians; non-Born–Oppenheimer calculations



### 1. Introduction

Experimental measurements of the frequencies and intensities corresponding to different isotopes of an atomic system may be useful in determining the isotope abundances in various environments both on Earth and in various regions of interstellar space. As the shifts of the spectral lines corresponding to the different isotopes of an atom decrease with the atomic number, it requires an increasingly higher resolution of the spectrum-measuring technique to discern between the lines of different isotopes. The question we attempt to answer in this work concerns the size of the isotope shifts of spectral lines of the ground and excited  $^3P^e$  (even parity) states of the three stable isotopes of the carbon atom ( $^{12}\text{C}$ ,  $^{13}\text{C}$ , and  $^{14}\text{C}$ ), which is the fourth most abundant element in the universe by mass.

The isotope shifts of carbon are being determined in this work based on quantum mechanical calculations that adopt the method described in our previous papers [1, 2]. In this approach, the seven particles that form the carbon atom (i.e. the nucleus and six electrons) are treated on an equal footing. This requires that, at the first step, the operator representing the kinetic energy of the centre-of-mass is separated out from the total non-relativistic Hamiltonian,  $\hat{H}$ , representing the atom. This separation, which is briefly described below, results in the total laboratory frame Hamiltonian of the system splitting into the centre-of-mass Hamiltonian,  $\hat{H}_{\text{CM}}$ , and the internal Hamiltonian,  $\hat{H}_{\text{int}}$ , that describes the internal state of the atom.  $\hat{H}_{\text{int}}$  explicitly depends on the mass of the nucleus. We use it in the present work to determine the nonrelativistic energies of the ground and the

five lowest  $^3P^e$  excited states of  $^{12}\text{C}$ ,  $^{13}\text{C}$ , and  $^{14}\text{C}$  isotopes. In the calculations, the wave functions of the considered states are expanded in terms of all-particle symmetry-adapted explicitly correlated Gaussian functions (ECGs). The ECGs are described in the next section.

## 2. The method used in the calculations

### 2.1. The internal nonrelativistic Hamiltonian

Let us consider an isolated atom formed by  $N$  particles (i.e. a nucleus and  $n = N-1$  electrons. In general, let the masses of the particles be denoted by  $\{M_i\}$  and their charges by  $\{Q_i\}$ . We start with the positions of the particles first described using the Cartesian coordinates in the laboratory frame,  $\{\mathbf{R}_i\}$ . The laboratory coordinates and the corresponding linear momenta of the particles are:

$$\mathbf{R} = \begin{bmatrix} \mathbf{R}_1 \\ \mathbf{R}_2 \\ \vdots \\ \mathbf{R}_N \end{bmatrix} = \begin{bmatrix} X_1 \\ Y_1 \\ Z_1 \\ \vdots \\ Z_N \end{bmatrix}, \quad \mathbf{P} = \begin{bmatrix} \mathbf{P}_1 \\ \mathbf{P}_2 \\ \vdots \\ \mathbf{P}_N \end{bmatrix} = \begin{bmatrix} P_{x1} \\ P_{y1} \\ P_{z1} \\ \vdots \\ P_{zN} \end{bmatrix}. \quad (1)$$

In the laboratory frame, the nonrelativistic Hamiltonian of the atom is given by

$$\hat{H}(\mathbf{R}) = \sum_{i=1}^N \frac{\mathbf{P}_i^2}{2M_i} + \sum_{i=1}^N \sum_{j>i}^N \frac{Q_i Q_j}{|\mathbf{R}_i - \mathbf{R}_j|}. \quad (2)$$

The above Hamiltonian can be separated into a 3D problem of the motion of the centre-of-mass of the atom and an  $(3N-3)$ -dimensional internal problem of the motions of the particles forming the atom with respect to each other. The separation of the two problems is achieved by transforming Hamiltonian (2) to a new coordinate system whose first three coordinates,  $\mathbf{r}_0$ , are the lab-frame coordinates of the centre-of-mass and the remaining  $3N-3$  coordinates are the internal Cartesian coordinates,  $\mathbf{r}_i$  ( $i = 1, \dots, N-1$ ). These coordinates are the relative coordinates of the electrons (i.e. particles 2 to  $N$  with respect to particle 1, the nucleus).

The separation of  $\hat{H}_{\text{tot}}$  into  $\hat{H}_{\text{CM}}$  and  $\hat{H}_{\text{int}}$  is rigorous. In the new coordinate system, Hamiltonian (2) becomes:

$$\begin{aligned} \hat{H}_{\text{tot}}(\mathbf{r}_0, \mathbf{r}) = & -\frac{1}{2} \frac{1}{M_{\text{tot}}} \nabla_{\mathbf{r}_0}^2 - \frac{1}{2} \sum_i^n \frac{1}{\mu_i} \nabla_{\mathbf{r}_i}^2 \\ & - \frac{1}{2} \sum_{i \neq j}^n \frac{1}{m_0} \nabla'_{\mathbf{r}_i} \nabla_{\mathbf{r}_j} + \sum_{i < j}^n \frac{q_i q_j}{r_{ij}} + \sum_{i=1}^n \frac{q_0 q_i}{r_i}, \end{aligned} \quad (3)$$

where  $\nabla_{\mathbf{r}_i}$  is the gradient vector expressed in terms of the  $x_i$ ,  $y_i$ , and  $z_i$  coordinates of vector  $\mathbf{r}_i$ ,  $r_{ij} =$

$|\mathbf{r}_i - \mathbf{r}_j| = |\mathbf{R}_{i+1} - \mathbf{R}_{j+1}|$ ,  $r_{0i} \equiv r_i = |\mathbf{r}_i| = |\mathbf{R}_{i+1} - \mathbf{R}_1|$ ,  $q_i = Q_{i+1}$  ( $i = 0, \dots, n$ ) are the particle charges,  $\mu_i = m_0 m_i / (m_0 + m_i)$  is the reduced mass of the  $i$ th electron,  $M_{\text{tot}}$  is the total mass of all particles in the system,  $m_0$  is the mass of the nucleus, and  $m_i = M_{i+1}$ . For the nuclear mass we adopted the following values:  $m_0(^{12}\text{C}) = 21868.663850 m_e$ ,  $m_0(^{13}\text{C}) = 23697.667827 m_e$ , and  $m_0(^{14}\text{C}) = 25520.350606 m_e$ , where  $m_e = 1$  is the mass of an electron. These were derived from the experimental values of atomic masses [3]. The prime symbol in Equation (3) is used to denote the vector/matrix transposition.

In the new coordinate system, the laboratory frame Hamiltonian (3) becomes a sum of the operators representing the kinetic energy of the centre-of-mass motion,  $\hat{H}_{\text{CM}}(\mathbf{r}_0)$ , and the internal Hamiltonian,  $\hat{H}_{\text{int}}(\mathbf{r})$ :

$$\hat{H}_{\text{tot}}(\mathbf{r}_0, \mathbf{r}) = \hat{H}_{\text{CM}}(\mathbf{r}_0) + \hat{H}_{\text{int}}(\mathbf{r}), \quad (4)$$

where  $\mathbf{r}$  is a  $3n$ -component column vector. Its first three components are coordinates  $\mathbf{r}_1$ , the next three are  $\mathbf{r}_2$ , etc. In the present work, we are only concerned with the bound states of the system represented by the eigenvalues and eigenfunctions of  $\hat{H}_{\text{int}}$ .

Upon examining the form of the internal Hamiltonian, one can see that it describes a system of  $n$  pseudo-electrons with masses equal to reduced masses  $\mu_i$  and charges  $q_i$  ( $i = 1, \dots, n$ ) moving in the central field of the charge of the nucleus,  $q_0$ , located in the centre of the internal coordinates system. We call the moving particles pseudo-electrons because, while their charges are still equal to  $-1$ , their masses are not the original electron masses but the reduced masses,  $\mu_i$ . Note that the pseudo-electrons become slightly ‘heavier’ as the mass of the nucleus increases in the  $^{12}\text{C}$ – $^{13}\text{C}$ – $^{14}\text{C}$  isotope series. In  $\hat{H}_{\text{int}}$ , the motion of the pseudo-electrons are correlated due to their repulsive interaction with each other via the Coulomb potential. In addition, their motion is also correlated (coupled) through the mass-polarisation term,  $-\frac{1}{2} \sum_{i \neq j}^n \frac{1}{m_0} \nabla'_{\mathbf{r}_i} \nabla_{\mathbf{r}_j}$ .

### 2.2. Variational method and ECGs basis functions

The calculations are performed in the framework of the Rayleigh-Ritz variational method. The spatial part of the wave function of the system,  $\Psi$ , is approximated as a linear combination of  $K$  ECGs  $\phi_k$ :

$$\Psi(\mathbf{r}) = \sum_{k=1}^K \mathbf{c}_k \hat{Y} \phi_k(\mathbf{r}), \quad (5)$$

where  $\mathbf{c}_k$  are the linear variational parameters, and  $\hat{Y}$  is a permutational symmetry projector represented as a

linear combination of permutational operators. In the present calculations of the carbon atom,  $\hat{Y}$  is chosen as

$$\begin{aligned}\hat{Y} = & (1 + \hat{P}_{45})(1 + \hat{P}_{67})(1 - \hat{P}_{46})(1 - \hat{P}_{24} - \hat{P}_{26}) \\ & (1 - \hat{P}_{32} - \hat{P}_{36} - \hat{P}_{34})(1 - \hat{P}_{57}),\end{aligned}$$

where we number particles in such a way that particle 1 is the nucleus and particles 2–7 are the electrons, and  $\hat{P}_{ij}$  permutes the labels of electrons  $i$  and  $j$  (for more information see Section 3.5 in Ref. [2]). As the Hamiltonian is spin-independent, the calculations can be carried out using the spin-free formalism [4, 5]. In this formalism, basis functions are constructed to have certain permutational symmetry. In practice, this results in calculating the overlap and Hamiltonian matrix elements where the ket functions are operated on with the operator  $\hat{Y}^\dagger \hat{Y}$  (the dagger stands for conjugate). An appropriate Young projection operator  $\hat{Y}$  can be derived using a Young tableaux suitable for the state under consideration [1, 2].

Minimising the energy expectation value with respect to the expansion coefficients  $c_k$  involves solving the generalised eigenvalue problem:

$$\mathbf{H}\mathbf{c} = \epsilon \mathbf{S}\mathbf{c}, \quad (6)$$

where  $\epsilon$  and  $\mathbf{c}$  are the eigenvalue and eigenvector corresponding to a particular excited state, while  $\mathbf{H}$  and  $\mathbf{S}$  are  $K \times K$  Hamiltonian and overlap matrices with the elements  $H_{kl} = \langle \phi_k | \hat{H}_{\text{int}} | \phi_l \rangle$  and  $S_{kl} = \langle \phi_k | \phi_l \rangle$ .

The computational time for calculating a matrix element of each of the two matrices is, in general, proportional to  $n^3$ , as it involves matrix operations such as inversion and multiplication. The time is also proportional to the product of the factorials of the numbers of identical particles in the system. In the calculations of the carbon atom, where the only identical particles are electrons, this factor is  $6! = 720$ . The factor is equal to the number of terms in the permutation symmetry operator  $\hat{Y}^\dagger \hat{Y}$  that needs to be applied to the ket basis function.

After computing the  $\mathbf{H}$  and  $\mathbf{S}$  matrix elements, the generalised eigenvalue problem (6) is solved. Depending on the size of the basis  $K$  it may also make a sizable contribution to the overall cost of the calculation despite using a quick solver involving finding only a single eigenvalue and the corresponding eigenvector.

The atom-like symmetry of the internal atomic Hamiltonian, (3), requires that the spatial basis functions used to expand the wave function of such a Hamiltonian need to be one-centre functions that form a basis for irreducible representations of the  $SO(3)$  group of rotations. To achieve high accuracy in the computations we use explicitly-correlated single-centre all-particle Gaussian (ECG) functions. We have used various forms of ECGs in

very accurate non-BO calculations of stationary atomic bound states for over two decades [2]. The simplest ECG with real nonlinear parameters suitable for computing  $S$  states of an  $n$ -electron atom is:

$$\phi_k(\mathbf{r}) = \exp[-\mathbf{r}' \mathbf{A}_k \mathbf{r}] \quad (\text{S - ECG}), \quad (7)$$

where  $\mathbf{r}$  is vector of  $3n$  internal Cartesian coordinates of the electrons and  $\mathbf{A}$  is a  $3n \times 3n$  real symmetric positive-definite matrix of the nonlinear parameters.  $\mathbf{A}_k$  has the following block structure:  $\mathbf{A}_k = A_k \otimes I_3$ , where  $A_k$  is a  $n \times n$  real dense symmetric positive-definite matrix and  $I_3$  is a  $3 \times 3$  identity matrix, while the symbol  $\otimes$  denotes the Kronecker product. Such representation of the matrix  $\mathbf{A}_k$  ensures that the exponent of the basis function is invariant with respect to 3D rotations.

The atomic system considered here, the carbon atom, has two  $p$ -electrons and  $n-2$   $s$ -electrons. The standard procedure for adding angular momenta is applied to construct ECGs for such a case [1, 2]. As in this work we consider  $^3P$  states, the calculations are performed with ECGs representing the total angular momentum  $L = 1$  and its projection on the  $z$ -axis  $M_L = 0$ . The ECGs for such states are constructed by multiplying  $S$ -ECGs by a Cartesian angular factor  $(x_i y_j - x_j y_i)$  [1, 2]. Thus, the ECGs used in this work to expand the spatial part of the wave functions of the calculated ground and excited  $^3P$  states of the carbon atom are given by

$$\phi_k = (x_{i_k} y_{j_k} - x_{j_k} y_{i_k}) \exp[-\mathbf{r}' (A_k \otimes I_3) \mathbf{r}], \quad (8)$$

where  $i_k$  and  $j_k$  are labels of the  $p$ -electrons. Subscript  $k$  reflects the fact that matrix  $A_k$  and electron labels  $i_k$  and  $j_k$  are variational parameters that are unique for each basis function.

It should be noted that basis functions (8) are of even parity and can be used to expand the wave functions of even parity states only. To represent odd parity states (not considered in this work) a different type of ECGs must be adopted.

To make function (8) square integrable it is convenient to represent  $A_k$  in a Cholesky factored form as  $A_k = L_k L_k'$ , where  $L_k$  is a lower triangular matrix. With this,  $\phi_k$  is automatically square integrable regardless of the values of the  $L_k$  matrix elements. The convenience of using the Cholesky representation of  $A_k$  comes in the variational minimisation of the energy with respect to the matrix elements of  $L_k$ . With no constraints imposed on these elements, their optimisation can be carried out without any restrictions. Such restrictions would be necessary if the optimisation parameters were the  $A_k$  matrix elements.

### 2.3. Total energy and energy gradient

The optimisation of the  $L_k$  Gaussian parameters in this work is performed through the minimisation of the Rayleigh-Ritz variational energy functional.

The minimisation with respect to the  $c_k$  coefficients leads to a secular Equation (6). The lowest-energy solutions of the secular equation represent the ground state and the higher-energy solutions represent excited states. All of them remain upper bounds to the corresponding exact energies.

In the minimisation of the Rayleigh-Ritz functional with respect to the nonlinear parameters of ECGs we adopt a procedure that employs analytic derivatives of the functional with respect to the parameters (the term analytic here means that the gradient is not obtained by applying the finite-difference formulas). Let  $\alpha_t$  be a vector of the nonlinear parameters of basis function  $\varphi_t$  (the parameters are the unique matrix elements of  $L_t$ ). As the  $t$ th row and  $t$ th column of matrices  $H$  and  $S$  depend on  $\alpha_t$ , the derivative of any element belonging to that row or that column of either of the two matrices can be written as:

$$\frac{\partial H_{kl}}{\partial \alpha_t} = \frac{\partial H_{kl}}{\partial \alpha_t} (\delta_{kt} + \delta_{lt} - \delta_{kt}\delta_{lt}), \quad k, l, t = 1 \dots K, \quad (9)$$

and

$$\frac{\partial S_{kl}}{\partial \alpha_t} = \frac{\partial S_{kl}}{\partial \alpha_t} (\delta_{kt} + \delta_{lt} - \delta_{kt}\delta_{lt}), \quad k, l, t = 1 \dots K. \quad (10)$$

Using the above, the derivative of the total energy,  $\varepsilon$ , with respect to the parameters  $\alpha_t$  is:

$$\begin{aligned} \frac{\partial \varepsilon}{\partial \alpha_t} &= c_t^* \sum_{l=1}^K c_l \left( \frac{\partial H_{tl}}{\partial \alpha_t} - \varepsilon \frac{\partial S_{tl}}{\partial \alpha_t} \right) \\ &\quad + c_t \sum_{l=1}^K c_l^* \left( \frac{\partial H_{lt}}{\partial \alpha_t} - \varepsilon \frac{\partial S_{lt}}{\partial \alpha_t} \right) \\ &\quad - c_t c_t^* \left( \frac{\partial H_{tt}}{\partial \alpha_t} - \varepsilon \frac{\partial S_{tt}}{\partial \alpha_t} \right) \\ &= 2\Re \left[ c_t^* \sum_{l=1}^K c_l \left( \frac{\partial H_{tl}}{\partial \alpha_t} - \varepsilon \frac{\partial S_{tl}}{\partial \alpha_t} \right) \right] \\ &\quad - c_t c_t^* \left( \frac{\partial H_{tt}}{\partial \alpha_t} - \varepsilon \frac{\partial S_{tt}}{\partial \alpha_t} \right). \end{aligned} \quad (11)$$

By calculating such derivatives for all nonlinear parameters  $\alpha_t$ , the complete energy gradient is obtained. The use of the analytic gradient in the minimisation of the Rayleigh-Ritz functional significantly accelerates the speed of calculations.

### 3. Results

The approach briefly outlined in the previous section is implemented in a computer program written in FORTRAN using the MPI (Message Passing Interface) protocol that enables parallelism in the calculation [1, 2]. An ECG basis set is generated separately for each of the six lowest  $^3P$  states of  $^{12}\text{C}$  considered in this work. First, the basis set for the lowest state is grown from a small number of randomly selected ECGs to the final number of basis functions. The growing process involves adding ECGs one-by-one and optimising their nonlinear parameters with the use of the analytic gradient.

After a certain number of ECGs is added to the basis set, the whole set is reoptimised again using the one-function-at-a-time approach. After a certain number of ECGs is generated for the ground  $^3P$  state, the basis set is used as the starting set for the calculation of the second lowest  $^3P$  state of  $^{12}\text{C}$ . The procedure continues until six states for this system are calculated. Next, the basis sets generated for the lowest  $^3P$  states of  $^{12}\text{C}$  are used to calculate the energies of six states of  $^{13}\text{C}$  and  $^{14}\text{C}$ .

For the two latter isotopes, no reoptimisation of the nonlinear parameters are performed and only the linear expansion coefficients  $c_k$  are adjusted to account for the change of the nuclear mass, this approach is justified because the wave function of the atom undergoes a relatively small change when one nuclear mass value is replaced with another (as long as it remains much larger than the mass of the electron). The growing of the basis sets for  $^{12}\text{C}$  is stopped when the convergence of the results appears sufficiently tight to determine the isotope shifts of the interstate transition frequencies of  $^{12}\text{C}$ ,  $^{13}\text{C}$ , and  $^{14}\text{C}$  with adequate accuracy.

It should be emphasised that the errors in the total energies (which always shift up, according to the variational principle) obtained in our calculations for different isotopes are correlated. This is because the same basis is used in the calculation of the same state of different isotopes. As a result, the relative error in the isotopic shift is roughly of the same order of magnitude as the relative error of the total energy.

In Table 1, nonrelativistic energies obtained for the ground  $2s^2 2p^2$   $^3P$  state of  $^{12}\text{C}$ ,  $^{13}\text{C}$ , and  $^{14}\text{C}$  are shown for three different basis set sizes (1100, 1200, and 1300 for the first two and the last two states, and 1200, 1300, and 1400 for the middle two states). For each state, the energies are extrapolated to the infinite number of ECGs. The extrapolated values are also shown in the table along with the estimated uncertainties (given in parentheses) due to the basis truncation. More elaboration about the extrapolation technique can be found in our previous paper [7]. As expected, the basis set incompleteness error increases

**Table 1.** Convergence of the nonrelativistic energies (in atomic units) for the considered six lowest  $^3P$  states of  $^{12}\text{C}$ ,  $^{13}\text{C}$ , and  $^{14}\text{C}$  with the number of ECGs obtained in this work.

State	Basis	$^{12}\text{C}$	$^{13}\text{C}$	$^{14}\text{C}$
$2s^2 2p^2$	1100	−37.841891	−37.842023	−37.842136
	1200	−37.842047	−37.842179	−37.842292
	1300	−37.842170	−37.842302	−37.842415
	$\infty$	−37.84253 ± 0.00036	−37.84266 ± 0.00036	−37.84278 ± 0.00036
ECG lobes [6]	$\infty$	−37.843194 ± 0.000004	−37.843326 ± 0.000004	−37.843439 ± 0.000004
	1100	−37.515935	−37.516067	−37.516180
$2s^2 2p\ 3p$	1200	−37.516168	−37.516301	−37.516414
	1300	−37.516334	−37.516466	−37.516579
$2s^2 2p\ 4p$	$\infty$	−37.51681 ± 0.00048	−37.51695 ± 0.00048	−37.51706 ± 0.00048
	1200	−37.46970	−37.46983	−37.46994
	1300	−37.47008	−37.47021	−37.47033
	1400	−37.47027	−37.47041	−37.47052
	$\infty$	−37.47084 ± 0.00057	−37.47098 ± 0.00057	−37.47109 ± 0.00057
$2s^2 2p\ 5p$	1200	−37.45016	−37.45029	−37.45040
	1300	−37.45076	−37.45089	−37.45100
	1400	−37.45095	−37.45108	−37.45120
	$\infty$	−37.45150 ± 0.00055	−37.45164 ± 0.00055	−37.45175 ± 0.00055
$2s^2 2p\ 6p$	1100	−37.4327	−37.4329	−37.4330
	1200	−37.4356	−37.4357	−37.4359
	1300	−37.4374	−37.4376	−37.4377
	$\infty$	−37.4429 ± 0.0054	−37.4430 ± 0.0054	−37.4431 ± 0.0054
$2s^2 2p\ 7p$	1100	−37.4121	−37.4122	−37.4124
	1200	−37.4185	−37.4187	−37.4188
	1300	−37.4222	−37.4224	−37.4225
	$\infty$	−37.4333 ± 0.0111	−37.4334 ± 0.0111	−37.4335 ± 0.0111

with the level of the excitation. It can be seen that the finite value of the nuclear mass affects the sixth digit of the energy values. As expected, for each of the six states, the energy of the heaviest isotope,  $^{14}\text{C}$ , is the lowest while the energy of the lightest isotope,  $^{12}\text{C}$  is the highest. It should be noted that a majority of the accurate studies of the carbon atom have employed the Born–Oppenheimer approximation (i.e. the calculations have been performed for  $^{\infty}\text{C}$ ) with the Configuration Interaction [8–11], Multiconfiguration Dirac–Hartree–Fock [11], and Monte-Carlo [12–14] methods. Also, the account of the non-BO effects within these methods are usually limited to the mass polarisation terms which in all aforementioned works have been omitted. Thus, the results obtained with these methods are not included in the table. The only previous high-accuracy calculations on the ground states of the carbon atom were performed by Strasburger using ECG lobe functions [6]. He used 5896 of these functions in the wave function expansion, leading to results with a high degree of accuracy. The values calculated with the ECG lobes have been shown in Table 1. Also, it should be noted that Strasburger did not calculate any excited states within the two spin symmetries he considered in his work, i.e. the triplet and quintuplet symmetries. Thus, it is not possible to calculate the transition energies using his results.

The nonrelativistic transition energies ( $\Delta E_{\text{nr}}$ ) for  $2s^2 2p^1 np^1\ 3P$  ( $n = 3 – 7$ ) states of carbon atom isotopes  $^{12}\text{C}$ ,  $^{13}\text{C}$ , and  $^{14}\text{C}$ , as well as of the natural mixture

(corresponding to the 98.93% and 1.07% abundance by mass of  $^{12}\text{C}$  and  $^{13}\text{C}$ , respectively [15]) with respect to the ground  $2s^2 2p^2\ 3P$  state are shown in Table 2. The transition energies are calculated using the energy values extrapolated to the infinite basis set limits taken from Table 1. The calculated transitions for the natural mixture are compared in the table with the experimental transitions taken from Ref. [15], which we assume also corresponds to the natural mixture. The comparison indicates that the natural mixture transition energies calculated in this work are increasingly more off from the experimental values as the excitation level increases. This is expected as the numbers of ECGs used in the present calculations are relatively small. Our recent calculations for five-electron boron [7] and carbon-ion [16] atomic systems indicate that well over 10 000 ECGs are needed to achieve adequate convergence of the energies for low-lying states to obtain transition energies within the uncertainties of the current experimental data. In the calculations of the low-lying states of the carbon atom, the number of ECGs that needs to be employed in order to reach comparable accuracy of the energy as for B and  $\text{C}^+$  is likely to exceed 20 000. We should also mention that previous calculations (see Table IV in Ref. [17]) using the ECG ansatz for  $^2\text{S}$  states of  $\text{C}^+$  ion have shown that the contribution of the relativistic and quantum electrodynamics (QED) effects, which are not considered in the present work, can be quite significant. In spite of the small size of the basis sets employed, it is expected that including the

**Table 2.** The nonrelativistic transition energies ( $\Delta E_{\text{nr}}$ ) for  $n\ 3P$  ( $n = 2 - 7$ ) states of the carbon atom isotope ( $^{12}\text{C}$ ,  $^{13}\text{C}$ , and  $^{14}\text{C}$ ) and the natural Earth mixture (NM; corresponding to the 98.93% and 1.07% abundance by mass of  $^{12}\text{C}$  and  $^{13}\text{C}$ , respectively [15]) calculated with respect to the ground  $2s^2 2p^2\ 3P$  state.

Basis	$^{12}\text{C}$	$^{13}\text{C}$	$^{14}\text{C}$	NM
$2s^2 2p^2 \rightarrow 2s^2 2p\ 3P$				
1100	71539.13	71539.10	71539.07	71539.13
1200	71522.14	71522.10	71522.07	71522.14
1300	71512.79	71512.76	71512.73	71512.79
$\infty$	$71495 \pm 18$	$71494 \pm 18$	$71494 \pm 18$	$71495 \pm 18$
Experimental				$71345.34 \pm 0.0023$
$2s^2 2p^2 \rightarrow 2s^2 2p\ 4P$				
1100	81686.90	81686.89	81686.88	81686.90
1200	81636.87	81636.86	81636.85	81636.87
1300	81621.79	81621.78	81621.77	81621.79
$\infty$	$81593 \pm 29$	$81593 \pm 29$	$81593 \pm 29$	$81593 \pm 29$
Experimental				$81304.7159 \pm 0.0023$
$2s^2 2p^2 \rightarrow 2s^2 2p\ 5P$				
1100	85975.19	85975.19	85975.18	85975.19
1200	85877.86	85877.86	85877.85	85877.86
1300	85862.39	85862.39	85862.39	85862.39
$\infty$	$85833 \pm 29$	$85833 \pm 29$	$85833 \pm 29$	$85833 \pm 29$
Experimental				$85165.4024 \pm 0.0301$
$2s^2 2p^2 \rightarrow 2s^2 2p\ 6P$				
1100	89800.08	89800.05	89800.03	89800.08
1200	89201.91	89201.90	89201.88	89201.91
1300	88832.73	88832.72	88832.71	88832.73
$\infty$	$88120 \pm 714$	$88120 \pm 714$	$88120 \pm 714$	$88120 \pm 707$
Experimental				$87076.2980 \pm 0.0359$
$2s^2 2p^2 \rightarrow 2s^2 2p\ 7P$				
1100	94325.87	94325.81	94325.76	94325.87
1200	92948.86	92948.81	92948.77	92948.86
1300	92163.19	92163.15	92163.12	92163.19
$\infty$	$90701 \pm 1461$	$90701 \pm 1461$	$90701 \pm 1461$	$90701 \pm 1446$
Experimental				$88162.4036 \pm 0.0584$

Note: The transition energies are calculated using the energy values extrapolated to infinite basis set limits taken from Table 1 (the extrapolation approach is described in Ref. [7]). The uncertainties due to the basis truncation error are shown in the parentheses. The numerical values in the parentheses represent the uncertainties affecting the last significant digit(s) shown in the table. The calculated transitions are compared with the experimental transitions taken from Ref. [15]. All entries are in units of  $\text{cm}^{-1}$ .

relativistic and QED corrections in the calculations may improve the results considerably.

Even though the number of ECGs used in the present calculations (1300–1400 ECGs) is by far smaller than that, we will show that, the calculated isotope shifts of the interstate transition energies are converged well enough to provide reasonably good estimates of this property. Our previous non-Born–Oppenheimer calculations on atomic species (for example see the helium [18] and lithium [19] calculations) have demonstrated that optimising the linear parameters of a basis set for each state suffices to obtain nonrelativistic energies with the same level of accuracy for all isotopes. So, we expect that the calculated isotope shifts have roughly the same relative accuracy as that of the nonrelativistic energy.

Table 3 shows the isotope shifts for the transitions from the excited  $2s^2 2p^1\ np^1\ (3P)$ ,  $n = 3, \dots, 7$ , states of the carbon atom isotopes ( $^{12}\text{C}$ ,  $^{13}\text{C}$ , and  $^{14}\text{C}$ ) to the ground  $2s^2 2p^2\ (3P)$  state. The calculated energies for the excited states of  $^{12}\text{C}$ ,  $^{13}\text{C}$ , and  $^{14}\text{C}$  are taken from Table 1. The ground-state energy is determined as the average of the calculated ground-state energies over the abundance of the naturally occurring isotopes (98.93% and 1.07% by mass for  $^{12}\text{C}$  and  $^{13}\text{C}$ , respectively [15]). Using this ground state energy the isotope energy shifts are calculated by subtracting this energy from the calculated excited state energies obtained for  $^{12}\text{C}$ ,  $^{13}\text{C}$ , and  $^{14}\text{C}$ . These were obtained for the basis set sizes of 1100, 1200, and 1300, as shown in Table 3. For each isotope and transition considered in this work, the isotope shifts are extrapolated to the infinite basis set limit and the

**Table 3.** The isotopic shift in energy for five transitions from the  $2s^2 2p^1 np^1 \ ^3P$ ,  $n = 3, \dots, 7$  states of the carbon atom isotopes ( $^{12}\text{C}$ ,  $^{13}\text{C}$ , and  $^{14}\text{C}$ ) to the ground  $2s^2 2p^2 \ ^3P$  state.

	$^{12}\text{C}$	$^{13}\text{C}$	$^{14}\text{C}$
$2s^2 2p^2 \rightarrow 2s^2 2p 3p$			
1100	0.00035837	-0.033134	-0.061732
1200	0.00035873	-0.033167	-0.061792
1300	0.00035884	-0.033178	-0.061815
$\infty$	$0.00035901 \pm 0.00000017$	$-0.033193 \pm 0.000015$	$-0.061862 \pm 0.000047$
$2s^2 2p^2 \rightarrow 2s^2 2p 4p$			
1100	0.000126	-0.01163	-0.02166
1200	0.000121	-0.01117	-0.02080
1300	0.000111	-0.01030	-0.01918
$\infty$	$0.000099 \pm 0.000012$	$-0.00917 \pm 0.00113$	$-0.01709 \pm 0.00210$
$2s^2 2p^2 \rightarrow 2s^2 2p 5p$			
1100	0.000053	-0.00487	-0.00906
1200	0.000034	-0.00311	-0.00578
1300	0.000025	-0.00230	-0.00427
$\infty$	$0.000014 \pm 0.000011$	$-0.00126 \pm 0.00104$	$-0.00233 \pm 0.00194$
$2s^2 2p^2 \rightarrow 2s^2 2p 6p$			
1100	0.000260	-0.0240	-0.0447
1200	0.000202	-0.0187	-0.0348
1300	0.000119	-0.0110	-0.0204
$\infty$	$0.000012 \pm 0.000106$	$-0.0011 \pm 0.0098$	$-0.0021 \pm 0.0183$
$2s^2 2p^2 \rightarrow 2s^2 2p 7p$			
1100	0.000630	-0.0583	-0.1085
1200	0.000520	-0.0480	-0.0895
1300	0.000388	-0.0359	-0.0668
$\infty$	$0.000222 \pm 0.000166$	$-0.0205 \pm 0.0153$	$-0.0383 \pm 0.0286$

Note: The ground-state energy is determined as the average of the calculated ground-state energies over the abundance of the naturally occurring isotopes (98.93% and 1.07% by mass for  $^{12}\text{C}$  and  $^{13}\text{C}$ , respectively [15]). The extrapolated values have been estimated using the same procedure as in Ref. [7]. The uncertainties due to the basis truncation error for the values obtained from extrapolation to an infinite number of ECGs are shown in parentheses. The numerical values in the parentheses represent the uncertainties affecting the last reported significant digit(s). All entries are in units of  $\text{cm}^{-1}$ .

values obtained from the extrapolation are also shown in Table 3.

Let us examine the convergence of the isotopic shift of the energy in the table. As one can see the convergence becomes increasingly worse with the excitation level. For the  $2s^2 2p^2 \rightarrow 2s^2 2p 3p$  transition the shifts are converged to 2-3 significant figures for all three isotopes. For the next two transitions, perhaps 1-2 figures are converged and for the following two only the sign of the shifts is correctly reproduced. We should note that the isotope shifts for  $^{12}\text{C}$  calculated with respect to the abundance-averaged median is the smallest because for this most abundant isotope the energy levels are close to the energy levels of the median. Also, we should note that the isotope shifts for  $^{12}\text{C}$  are positive with respect to the median, while for  $^{13}\text{C}$  and  $^{14}\text{C}$  they are negative.

In the next step, the energies of the  $2s^2 2p^1 np^1, n = 3, \dots, 7$ ,  $^3P_J$ ,  $J = 0, 1$ , and 2, states of the carbon isotopes,  $^{12}\text{C}$ ,  $^{13}\text{C}$ , and  $^{14}\text{C}$ , with respect to the experimental values shown in the first row of the last column is

predicted by combining the isotope shifts obtained in the present calculations and the experimental energies taken from NIST ASD database [15] and shown in the last column of Table 4. It is assumed that these experimental energies correspond to the naturally occurring isotope mixture (with 98.93% and 1.07% by mass of the  $^{12}\text{C}$  and  $^{13}\text{C}$  isotopes, respectively [15]). It is also assumed that the spectral lines corresponding to different levels (i.e. different  $J$  values) of the same term, uniformly shift when going from one isotope to another. The table shows energies which are sums of the experimental energies and the corresponding calculated isotope energy shifts extrapolated to the infinite number of ECGs taken from Table 3. Upon examining the results shown in Tables 3 and 4, we can conclude that the isotope shifts for the two lowest transitions,  $2s^2 2p^2 \rightarrow 2s^2 2p 3p$  and  $2s^2 2p^2 \rightarrow 2s^2 2p 4p$  are perhaps large enough ( $0.06-0.01 \text{ cm}^{-1}$ ) and converged enough for the  $^{13}\text{C}$  and  $^{14}\text{C}$  isotopes to be visible in the high-resolution spectrum of the carbon atom.

**Table 4.** Predicted energies of the  $2s^2 2p^1 np^1$ ,  $n = 3, \dots, 7$   $^3P_J$ ,  $J = 0, 1$ , and 2 states of the carbon isotopes,  $^{12}\text{C}$ ,  $^{13}\text{C}$ , and  $^{14}\text{C}$ , with respect to the experimental values shown in the first row of the last column.

	$^{12}\text{C}$	$^{13}\text{C}$	$^{14}\text{C}$	Experiment
$2s^2 2p^2$				
$J = 0$	$0.00036 \pm 0.00130$	$-0.03319 \pm 0.00130$	$-0.06186 \pm 0.00130$	$0.0000000 \pm 0.0013$
$J = 1$	$16.4171 \pm 0.00130$	$16.3835 \pm 0.0013$	$16.3549 \pm 0.0013$	$16.4167 \pm 0.0013$
$J = 2$	$43.4138 \pm 0.00130$	$43.3803 \pm 0.0013$	$43.3516 \pm 0.0013$	$43.4135 \pm 0.0013$
$2s^2 2p^2 \rightarrow 2s^2 2p 3p$				
$J = 0$	$71352.54354 \pm 0.00025$	$71352.5343 \pm 0.0012$	$71352.5264 \pm 0.0021$	$71352.54344 \pm 0.00025$
$J = 1$	$71364.93606 \pm 0.00019$	$71364.9268 \pm 0.0011$	$71364.9189 \pm 0.0021$	$71364.93596 \pm 0.00019$
$J = 2$	$71385.410019 \pm 0.000012$	$71385.4008 \pm 0.0011$	$71385.3928 \pm 0.0021$	$71385.40992(0)$
$2s^2 2p^2 \rightarrow 2s^2 2p 4p$				
$J = 0$	$81311.05441 \pm 0.00030$	$81311.0531 \pm 0.0011$	$81311.0521 \pm 0.0020$	$81311.05440 \pm 0.0003$
$J = 1$	$81325.81078 \pm 0.00020$	$81325.8095 \pm 0.0011$	$81325.8084 \pm 0.0020$	$81325.81077 \pm 0.00020$
$J = 2$	$81344.05486 \pm 0.00011$	$81344.0536 \pm 0.0010$	$81344.0525 \pm 0.0019$	$81344.05485 \pm 0.00011$
$2s^2 2p^2 \rightarrow 2s^2 2p 5p$				
$J = 0$	$85169.660 \pm 0.030$	$85169.659 \pm 0.032$	$85169.658 \pm 0.035$	$85169.660 \pm 0.03$
$J = 1$	$85188.96701 \pm 0.00041$	$85188.9659 \pm 0.0099$	$85188.965 \pm 0.018$	$85188.96700 \pm 0.0004$
$J = 2$	$85203.67561 \pm 0.00032$	$85203.6745 \pm 0.0099$	$85203.674 \pm 0.018$	$85203.67560 \pm 0.0003$
$2s^2 2p^2 \rightarrow 2s^2 2p 6p$				
$J = 0$	$87077.402 \pm 0.022$	$87077.381 \pm 0.027$	$87077.364 \pm 0.036$	$87077.402 \pm 0.022$
$J = 1$	$87103.134 \pm 0.019$	$87103.113 \pm 0.024$	$87103.096 \pm 0.034$	$87103.134 \pm 0.019$
$J = 2$	$87113.239 \pm 0.021$	$87113.218 \pm 0.026$	$87113.201 \pm 0.036$	$87113.239 \pm 0.021$
$2s^2 2p^2 \rightarrow 2s^2 2p 7p$				
$J = 0$	$88159.925 \pm 0.030$	$88160.67 \pm 0.17$	$88161.32 \pm 0.31$	$88159.930 \pm 0.03$
$J = 1$	$88192.335 \pm 0.030$	$88193.08 \pm 0.17$	$88193.73 \pm 0.31$	$88192.340 \pm 0.03$
$J = 2$	$88198.195 \pm 0.040$	$88198.94 \pm 0.17$	$88199.59 \pm 0.31$	$88198.200 \pm 0.04$

Note: The experimental energies shown in the last column are taken from NIST ASD [15]. It is assumed that these experimental energies correspond to the naturally occurring isotope mixture (with 98.93% and 1.07% by mass of the  $^{12}\text{C}$  and  $^{13}\text{C}$  isotopes, respectively [15]). The energies reported in the table are obtained by adding isotope shifts extrapolated to an infinite number of ECGs taken from Table 3 to the corresponding energies shown in the last column of the table. All entries are in units of  $\text{cm}^{-1}$ .

## 4. Summary

In this work, we describe a procedure for calculating isotope shifts of the spectral lines corresponding to the electronic states of the most common isotopes of the carbon atom. The procedure involves performing accurate quantum mechanical calculations of the energies corresponding to these spectral lines for different isotopes. In the case of the carbon atom considered in this work, the isotopes are  $^{12}\text{C}$ ,  $^{13}\text{C}$ , and  $^{14}\text{C}$  and the considered states are the  $2s^2 2p^1 np^1$  ( $^3P$ ),  $n = 2 - 7$ , states. The calculations are carried out using the variational method with the Hamiltonian explicitly dependent on the mass of the nucleus of the atom. The spatial part of the wave function of the atom is expanded in terms of all-electron explicitly correlated Gaussians and the nonlinear parameters of the Gaussians are extensively optimised using a procedure that employs the analytic energy gradient. The calculated isotope shifts of the energies are combined with the experimentally determined state energies to predict the positions of the spectral lines corresponding to different carbon isotopes. Based on the results, we conclude that future high resolution spectroscopic measurements may discern spectral lines corresponding to different isotopes of the carbon atom.

## Acknowledgments

The authors are grateful to the University of Arizona Research Computing for providing computational resources for this work.

## Disclosure statement

No potential conflict of interest was reported by the author(s).

## Funding

This work has been supported by Nazarbayev University [faculty development grant number 021220FD3651] and the National Science Foundation [grant number 1856702].

## References

- [1] K.L. Sharkey, S. Bubin and L. Adamowicz, *J. Chem. Phys.* **132** (18), 184106 (2010). doi:10.1063/1.3419931.
- [2] S. Bubin, M. Pavanello, W.C. Tung, K.L. Sharkey and L. Adamowicz, *Chem. Rev.* **113**, 36–79 (2013). doi:10.1021/cr200419d.
- [3] M. Wang, W. Huang, F. Kondev, G. Audi and S. Naimi, *Chin. Phys. C* **45** (3), 030003 (2021). doi:10.1088/1674-1137/abddaf.
- [4] M. Hamermesh, *Group Theory and Its Application to Physical Problems* (Addison-Wesley, Reading, MA, 1962).

- [5] R. Pauncz, *Spin Eigenfunctions* (Plenum, New York, 1979).
- [6] K. Strasburger, Phys. Rev. A. **99**, 052512 (2019). doi:10.1103/PhysRevA.99.052512.
- [7] I. Hornyák, S. Nasiri, S. Bubin and L. Adamowicz, Phys. Rev. A **104**, 032809 (2021). doi:10.1103/PhysRevA.104.032809.
- [8] A.W. Weiss, Phys. Rev. **162**, 71–80 (1967). doi:10.1103/PhysRev.162.71.
- [9] A. Bunge, J. Chem. Phys. **53** (1), 20–28 (2003). doi:10.1063/1.1673766.
- [10] M.B. Ruiz and R. Tröger, in *Novel Electronic Structure Theory: General Innovations and Strongly Correlated Systems, Advances in Quantum Chemistry*, edited by Philip E. Hoggan (Academic Press, Cambridge MA, 2018), Vol. 76, pp. 223–238.
- [11] W. Li, A.M. Amarsi, A. Papouli, J. Ekman and P. Jöns-son, Mon. Not. R. Astron. Soc. **502** (3), 3780–3799 (2021). doi:10.1093/mnras/stab214.
- [12] P. Seth, P.L. Ríos and R.J. Needs, J. Chem. Phys. **134** (8), 084105 (2011). doi:10.1063/1.3554625.
- [13] A. Sarsa, E. Buendía and F.J. Gálvez, J. Phys. B: At. Mol. Opt. Phys. **49** (14), 145003 (2016). doi:10.1088/0953-4075/49/14/145003.
- [14] S. Nasiri and M. Zahedi, Int. J. Quantum. Chem. **120** (11), e26187 (2020). doi:10.1002/qua.v120.11.
- [15] A.E. Kramida, Y. Ralchenko, J. Reader and NIST ASD Team, *NIST Atomic Spectra [Database] (ver. 5.11) [Online]*, 2023, <http://physics.nist.gov/asd>.
- [16] M. Stanke, A. Kędziora, S. Nasiri, L. Adamowicz and S. Bubin, Phys. Rev. A. **108**, 012812 (2023). doi:10.1103/PhysRevA.108.012812.
- [17] I. Hornyák, L. Adamowicz and S. Bubin, Phys. Rev. A. **102**, 062825 (2020). doi:10.1103/PhysRevA.102.062825.
- [18] S. Nasiri, S. Bubin and L. Adamowicz, in *Chemical Physics and Quantum Chemistry, Advances in Quantum Chemistry*, edited by Kenneth Ruud and Erkki J. Brändas (San Diego, CA, 2020), Vol. 81, pp. 143–166.
- [19] S. Nasiri, T. Shomenov, S. Bubin and L. Adamowicz, J. Phys. B. **54** (8), 085003 (2021). doi:10.1088/1361-6455/abee97.